Spinning the "Ferrous Wheel": The importance of the microbial community in an iron budget during the FeCycle experiment

R. F. Strzepek,[1] M. T. Maldonado,[2] J. L. Higgins,[3] J. Hall,[4] K. Safi,[4] S. W. Wilhelm,[3] and P. W. Boyd[5]

Received 17 February 2005; revised 29 September 2005; accepted 25 October 2005; published 17 December 2005.

[1] Several studies have shown the importance of the microbial community in specific aspects of the biogeochemical iron (Fe) cycle such as uptake or regeneration. During FeCycle, a 10-day study of Fe biogeochemistry within an unperturbed mesoscale in situ SF_6 labeled patch of HNLC waters, we investigated the role of both microzooplankton (herbivores and bacterivores) and viruses in regenerating Fe in the upper ocean. In summer 2003 we measured grazer-mediated Fe regeneration rates. The proportion of bacterial Fe released via grazing was severalfold greater than that mobilized from phytoplankton during herbivory. However, as the algal Fe pool (mainly *Synechococcus*) was severalfold larger than the bacterial pool, the absolute Fe regeneration rates were similar for both herbivores (17 pmol Fe L^{-1} d^{-1}) and bacterivores (20 pmol Fe L^{-1} d^{-1}). In all grazing experiments we observed that 90% (bacterivory) and 25% (herbivory) of the labeled Fe resided in the dissolved fraction after 24 hours. This trend has previously been reported in similar laboratory culture studies, which invoked the formation of dissolved, and/or colloidal metal ligands, associated with digestion, to make the released Fe less bioavailable. This explanation may not be valid for our study as another FeCycle experiment (Maldonado et al., 2005) demonstrated that resident phytoplankton could obtain Fe bound to a wide range of strong-binding ligands. In situ estimates of virally mediated Fe regeneration during FeCycle ranged from 0.4 to 28 pmol L^{-1} d^{-1}. It is not known why such a wide range of virally mediated regeneration rates was observed. Such variability prevented a direct comparison on the relative roles of grazers and viruses in Fe recycling. The rates of grazer-mediated regeneration accounted for 30% to >100% of the bacterial and phytoplankton Fe demand measured during FeCycle, indicating the key role of the microbial food web in Fe recycling.

Citation: Strzepek, R. F., M. T. Maldonado, J. L. Higgins, J. Hall, K. Safi, S. W. Wilhelm, and P. W. Boyd (2005), Spinning the ''Ferrous Wheel'': The importance of the microbial community in an iron budget during the FeCycle experiment, *Global Biogeochem. Cycles*, *19*, GB4S26, doi:10.1029/2005GB002490.

1. Introduction

[2] It is now well established that microbial communities are integral components of the complex foodwebs of pelagic oceanic waters [*Pomeroy*, 1974; *Azam et al.*, 1983]. Heterotrophic prokaryotes are adept at recycling dissolved organic matter within foodwebs via microbial grazers [*Azam et al.*, 1983]. Moreover, transformation of carbon, through grazing [*Schmidt et al.*, 1999], bacterial particle solubilization [*Bidle et al.*, 2002], and virus-mediated cell lysis [*Wilhelm and Suttle*, 1999] influences the elemental composition of biogenic particulates. Many studies have now clearly documented the key role of the microbial community in pelagic carbon cycling [*Ducklow and Carlson*, 1992], but less is known about how microbes influence the biogeochemical cycling of trace elements such as Fe [*Kirchman*, 1996].

[3] A large number of lab (reviewed by *Morel and Price* [2003]), shipboard (reviewed by *de Baar and Boyd* [1999]) and mesoscale Fe-enrichment [*Boyd*, 2004] experiments have highlighted the importance of Fe in a myriad of oceanic processes. These studies suggest that primary productivity in up to 50% of oceanic waters may be limited by the biological availability of Fe [*Moore et al.*, 2002]. However, in spite of the obviously important role for microbes in these environments, there have been relatively few studies focusing on the role of the microbial foodweb within the marine Fe cycle [*Kirchman*, 1996].

[1]National Institute of Water and Atmospheric Research (NIWA), Centre for Chemical and Physical Oceanography, Department of Chemistry, University of Otago, Dunedin, New Zealand.
[2]Department of Earth and Ocean Sciences, University of British Columbia, Vancouver, British Columbia, Canada.
[3]Department of Microbiology, University of Tennessee, Knoxville, Tennessee, USA.
[4]National Institute of Water and Atmosphere, Hamilton, New Zealand.
[5]National Institute of Water and Atmosphere Centre for Chemical and Physical Oceanography, Department of Chemistry, University of Otago, Dunedin, New Zealand.

0886-6236/05/2005GB002490$12.00

[4] The microbial foodweb is characterized by a tight coupling between prey (both heterotrophs and autotrophs) and predators (microzooplankton) [*Landry et al.*, 1993] that probably accounts for the constancy of algal stocks within Fe-limited HNLC (high nitrate low chlorophyll) waters [*Strom et al.*, 2000]. Indeed, the ecumenical iron hypothesis of *Morel et al.* [1991] concludes that such HNLC characteristics are due to iron-limited phytoplankton under grazer control. Within the microbial foodweb, both prokaryotic and eukaryotic autotrophs [e.g., *Brand*, 1991; *Wilhelm and Trick*, 1994; *Sandström et al.*, 2002], and heterotrophs such as bacteria [*Tortell et al.*, 1996] and microzooplankton [*Chase and Price*, 1997] have significant Fe demands, particularly the picoplankton [*Brand*, 1991; *Tortell et al.*, 1996]. Lab studies of Fe regeneration [*Hutchins and Bruland*, 1994; *Barbeau et al.*, 1996] demonstrated that grazers rapidly recycled Fe. Thus the high demand and recycling of Fe within the microbial foodweb was referred to as the "Ferrous Wheel" by *Kirchman* [1996].

[5] The findings from such lab studies were used to interpret biogeochemical field data from HNLC regions, such as the equatorial Pacific, where *Landry et al.* [1996] discussed the link between Fe cycling and new and regenerated production. A key need in better understanding the biogeochemical Fe cycle is for concurrent estimates of the pools and fluxes of new versus recycled Fe [*Fung et al.*, 2000]. Such estimates for the "Ferrous Wheel" also require an assessment of not only the role of grazers in Fe recycling but that of viruses. A recent study reports that Fe recycling in HNLC waters may be strongly driven by the virus-mediated lysis of bacterioplankton [*Poorvin et al.*, 2004]. Thus both grazers and viruses play a role in Fe regeneration.

[6] Previous attempts to estimate the magnitude of pools and fluxes of Fe within microbial foodwebs have relied heavily on laboratory data that have been applied to regions such as the HNLC subarctic Pacific [*Price and Morel*, 1998] or Sargasso Sea [*Tortell et al.*, 1999]. In only one case has a microbial Fe budget been constructed mainly from concurrent open ocean measurements [*Bowie et al.*, 2001]. However, Bowie et al. measured Fe uptake and subsequent recycling in HNLC Southern Ocean waters that had been intentionally perturbed with Fe enrichment. Here we quantify the magnitude of key Fe pools and fluxes (heterotrophic and autotrophic, viral and grazer), determine how they vary over time, and construct a "steady state" microbial Fe budget during FeCycle, a study of a mesoscale SF_6 labeled patch of unperturbed HNLC waters, to investigate the biogeochemical cycling of Fe [*Boyd et al.*, 2005].

2. Materials and Methods

2.1. Study Site

[7] FeCycle commenced on 2 February 2003 when $\sim$50 km^2 of HNLC ocean SE of New Zealand was labeled with the inert tracer SF_6 (i.e., no Fe was added) and the patch of water was followed for 10 days [*Boyd et al.*, 2005]. Water was sampled from the surface mixed layer (i.e., upper 45 m) at the patch center (defined by the highest SF_6 concentrations from daily mapping [*Boyd et al.*, 2005]). Water for all experiments was collected from either 10 or 20 m depth, depending on small daily changes in mixed layer depth (40–45 m), using a trace metal-clean Teflon diaphragm pumping system. Sampling commenced shortly after local dawn when nighttime convective overturn would result in a truly "mixed" layer for several hours [*Boyd et al.*, 2005].

2.2. Cell Enumeration and Biomass Determination

[8] Picophytoplankton (phytoplankton < 2 μm) and bacterial abundances were determined by Flow Cytometry (FACSCalibur) following procedures detailed by *Hall et al.* [2004]. Picophytoplankton samples were frozen in liquid nitrogen [*Lebaron et al.*, 1998] and were thawed immediately before counting, with Trucount™ beads (50 μL) being added to each sample as a tracer [*Hall et al.*, 2004]. Samples were run at Hi flow setting (60 μL min^{-1}) with a minimum of 1500 counts per sample following *Coroz et al.* [1999]. Both picoeukaryote and *Synechococcus* sp. abundances were then measured. Cell carbon for the former was determined by first assessing average spherical diameter by microscopy. Biovolume was then converted using the *Booth* [1988] conversion for phytoplankton <4 μm, 220 fg C μm^{-3}, to yield a factor of 920 fg C per picoeukaryote. For *Synechococcus* sp. 250 fg C cell^{-1} [*Li et al.*, 1992] was used to calculate cell carbon.

[9] Bacterial samples were frozen in liquid nitrogen and stained with SYBRII stain (Molecular Probes Inc.) at a concentration of 10^{-4} mol L^{-1} and then incubated in the dark for 10–15 min before being analyzed following procedures of *Lebaron et al.* [1998]. Just prior to analysis, 100 μL of Trucount™ beads were added to each sample as a tracer. Bacterial cell carbon was estimated to be 12.4 fg C cell^{-1} after *Fukuda et al.* [1998].

[10] Duplicate samples collected for nanoflagellate enumeration were size-fractionated through a 20-μm nylon mesh. The filtrate was then fixed 1:1 with ice-cold glutaraldehyde (2% final concentration) for 1 hour [*Sanders et al.*, 1989]. Fixed samples were filtered onto 0.8-μm black Nuclepore® filters, stained for 5 min with 2 mL primulin, rinsed with 2 mL Tris HCl, mounted on slides and stored frozen [*Bloem et al.*, 1986]. Nanoflagellates were counted under UV excitation using epifluorescence microscopy, and nanophytoflagellates were differentiated using chlorophyll *a* under blue light excitation. Note that we were unable to distinguish whether pigmented nanoflagellates were autotrophic or mixotrophic. Forty randomly selected fields were counted per filter. Nanoflagellate biovolumes were calculated using dimensions and approximated geometric shape [*Chang*, 1988], and calculated from measurements on >200 cells. Cell carbon for both phytotrophic and heterotrophic nanoflagellate (HNF) biomass was assumed to be 0.24 pg C μm^{-3} as reported by *Verity et al.* [1992] for nanophytoflagellates.

[11] Microzooplankton were identified to genus where possible and enumerated using microscopy [*James and Hall*, 1995] but with no differentiation of plastidic ciliates. Ciliate biomass was estimated from dimensions of 10–20 randomly chosen individuals of each taxon. Biovolumes were estimated from approximate geometric shapes and were converted to carbon using 0.19 pg C μm^{-3} [*Putt and Stoecker*, 1989].

2.3. Heterotrophic Bacterial Production

[12] Production was measured at 7 depths (3, 5, 8, 12, 20, 30 and 45 m) using the (Methyl- ^{3}H) thymidine method

modified for microcentrifuge [*Smith and Azam*, 1992]. The mean value of results obtained at 8 and 12 m are reported. Counts were corrected for quench by external standards. To estimate bacterial production we converted mol thymidine to gC using *Fuhrman and Azam*'s [1982] factor of 2.4×10^{18} per mol thymidine incorporated.

2.4. Microzooplankton Grazing and Algal Growth Rates

[13] Grazing and growth rates were determined using the dilution technique of *Landry and Hasset* [1982], as modified by *Gallegos et al.* [1996]. Water for dilution was gravity filtered through a prerinsed 0.2-μm Pall Gelman SuporCap™. The time lag between water collection and initiating experiments was 2 hours or less. Using acid-washed, 2.4-L polycarbonate bottles, <200 μm screened water was diluted with 0.2-μm filtrate to concentrations of 10%, 40%, 70%, and 100% (i.e., undiluted). All bottles were then placed in an on deck incubator with continuous seawater supply and covered with shade cloth (40% transmission of incident light). Incubations for all experiments were conducted in triplicate bottles for 24 hours.

[14] The dilution factor for each bottle was calculated by taking subsamples for <200 μm chlorophyll *a* at T_0 (time zero) and measuring the percentage of <200 μm chlorophyll *a* in each treatment. Size-fractionated chlorophyll *a* and picophytoplankton subsamples were also taken at T_{24} (24 hours after T_0) from all dilutions. To determine the growth rate of grazers, we measured heterotrophic nanoflagellate and ciliate abundances in the 100% treatment at T_0 and T_{24}. Size-fractioned chlorophyll *a* samples were obtained using prefiltration at 20 and 2 μm. Chlorophyll *a* was measured spectrofluorometrically after *Strickland and Parsons* [1972].

[15] Linear feeding kinetics were corrected for the growth of grazers during the incubation by dividing linear regression slopes by the relative geometric mean predator density (GMPD) after *Gallegos et al.* [1996],

$$\mathrm{GMPD} = [Z_0 Z_{\Delta t}]^{1/2} = Z_0 e^{\mu \Delta t/2};$$

dividing by Z_0 gives the GMPD as

$$e^{\mu \Delta t/2},$$

where Z = grazer biomass density, Δt = duration of incubation, and μ = predator-specific growth rate (day^{-1}). Division of the slopes by relative GMPD reduced the errors in estimating grazing rates to a range from +6 to −12%.

2.5. Virus Abundance

[16] Samples for bacterial and virus enumeration were preserved in glutaraldehyde (final concentration, 2.5%). For viral studies, acridine orange staining [*Hobbie et al.*, 1977] was used to enumerate bacteria. Bacterial counts obtained by microscopy were consistently 10–20% lower than those from flow cytometry. To determine virus abundance, sample water (0.8 mL) was collected onto 0.02-μm-porosity Anodisc filters (Whatman) and stained with SYBR Green 1 prior to enumeration of virus-like particles by epifluorescence microscopy [*Noble and Fuhrman*, 1998]. Samples with high virus abundance required dilutions: 10 or 100 μL of the sample were diluted with 790 or 700 μL, respectively, of sterile marine medium (ESAW, [*Berges et al.*, 2001]).

2.6. Lytic Burst Size of Visibly Infected Cells

[17] Whole water (40 mL) was preserved with glutaraldehyde (as above) and stored in the dark at 4°C. Samples were subsequently collected onto carbon-coated collodion (2%, Electron Microscopy Sciences) films atop 400-mesh electron microscope grids by centrifugation. Grids were then rinsed with sterile water and stained with 0.75% uranyl formate. The frequency of visibly infected bacteria cells (FVIC) and burst size were determined by transmission electron microscopy (Hitachi H-800) after *Weinbauer and Suttle* [1996]. For each sample, two grids were prepared, and at least 1000 bacterial cells were examined per grid for infection. Burst size was defined as the average number of viral particles in all visibly infected cells (VIC). This is likely the minimum burst size, as continuation of the lytic cycle may lead to increased virus particle abundance [*Weinbauer and Suttle*, 1996].

2.7. Virus Production and Virus-Induced Mortality Rate Estimates

[18] Production rates were estimated using the dilution approach of *Wilhelm et al.* [2002]. To assay virus production rates, the bacterial community from 450 mL of seawater was gently collected on 0.2-μm-porosity polycarbonate filter (47 mm diameter; Millipore®). This served to wash free extracellular virus particles from the sample. These cells were resuspended while maintaining the initial volume with ultra-filtered seawater (<30 KDa). Three 150-mL subsamples were transferred to individual 500-mL polycarbonate bottles and incubated at in situ temperature in the dark. A 4-mL sample was collected from each bottle every 2.5 hours, and preserved with glutaraldehyde (final concentration, 2.5%). Each incubation was limited to 10 hours to reduce the amount of virus production observed from new infections. Mean production rates (viruses $\mathrm{mL}^{-1}\ \mathrm{h}^{-1}$) were calculated from the reoccurrence of viruses in each replicate over time. Viral production rates were then multiplied by the bacterial cell quota for Fe (0.44 ag cell^{-1}) to calculate the rates of Fe regeneration by viral lysis of bacterial cells. This Fe quota was derived from the cell carbon conversion factor of *Fukuda et al.* [1998] multiplied by the heterotrophic bacteria Fe:C ratio of *Tortell et al.* [1996].

2.8. Phytoplankton Stocks and Production

[19] Estimates of stocks were derived from chlorophyll *a*. Samples were collected on 0.2-μm-porosity polycarbonate filters (47 mm diameter; Millipore®). Chlorophyll *a* was extracted and quantified following procedures of *Welschmeyer* [1994]. Carbon fixation rates were determined from in situ incubations of water samples collected at 10 m depth [*McKay et al.*, 2005].

2.9. Prey-Labeling Bacterivory and Herbivory Experiments

2.9.1. Prey Labeling

[20] Iron regeneration rates by microzooplankton feeding on either heterotrophic bacteria (0.2–0.8 μm) or phyto-

Table 1. Partitioning of Fe Within Size Fractions During Four Grazing Experiments (Bacterivory and Herbivory)[a]

Experiment	Initial Labeled Pool	Size-Fractionated Fe Distribution After 24 Hours With Grazers: Size Fraction (μm)	Size-Fractionated Fe Distribution After 24 Hours With Grazers: Fe Content (pmol L^{-1})	Biogenic Fe Pool, pmol L^{-1}	Flux From Fe Pool, pmol L^{-1} d^{-1}	Percent Liberated Via Grazing
Grazing 1, 10–12 Feb	Heterotrophic bacteria (0.2–0.8 μm)	<0.2 (dissolved)	13.0	17.8	16.6	93.0
		>2.0 (autotrophs)	1.9			
		0.8–2.0 (*Synechococcus*)	1.7			
		0.2–0.8 (het. bacteria)	1.2			
		sum of fractions	17.8			
Grazing 2, 11–13 Feb	Heterotrophic bacteria (0.2–0.8 μm)	<0.2 (dissolved)	12.0	18.7	16.3	87.0
		>2.0 (autotrophs)	1.4			
		0.8–2.0 (*Synechococcus*)	2.9			
		0.2–0.8 (het. bacteria)	2.4			
		sum of fractions	18.7			
Grazing 1, 10–12 Feb	Phytoplankton (0.8–8.0 μm)	<0.2 (dissolved)	13.9	60.3	15.1	25.0
		>2.0 (autotrophs)	19.0			
		0.8–2.0 (*Synechococcus*)	26.3			
		0.2–0.8 (het. bacteria)	1.2			
		sum of fractions	60.3			
Grazing 2, 11–13 Feb	Phytoplankton (0.8–8.0 μm)	<0.2 (dissolved)	11.7	65.6	14.9	22.6
		>2.0 (autotrophs)	16.6			
		0.8–2.0 (*Synechococcus*)	34.1			
		0.2–0.8 (het. bacteria)	3.1			
		sum of fractions	65.6			

[a]See Figure 3. Data on partitioning were used to derive biogenic Fe pools, and subsequently regeneration rates and the proportion of Fe liberated via bacterivory (defined as Fe not in the 0.2–0.8 μm bacterial size fraction after T_{24}, divided by the biogenic Fe pool) or herbivory (Fe not in the 0.8–8 μm size fraction after T_{24}, divided by the biogenic Fe pool).

plankton (0.8–8.0 μm) were determined with ^{55}Fe radiolabeled plankton incubation experiments, essentially as described in Table 5 of *Bowie et al.* [2001]. All sample manipulations were conducted in a laminar flow bench and all materials in contact with the samples were thoroughly acid-washed prior to use. Two independent experiments were initiated on day 4 and 5 of FeCycle. Seawater was collected cleanly (P. T. Croot et al., The importance of physical mixing processes for understanding iron biogeochemical cycling: FeCycle, submitted to *Global Biogeochemical Cycles*, 2005) (hereinafter referred to as Croot et al., submitted manuscript, 2005) from 10 m depth (~70% of the subsurface irradiance (0.5 m depth)) and dispensed in duplicate acid-washed 4-L polycarbonate bottles that were capped and sealed with Parafilm. Experiments were initiated by adding either 1 nmol L^{-1} ^{55}Fe (NEN Life Sciences) bound to 10 μmol L^{-1} EDTA (low Fe treatment) or 20 nmol L^{-1} total Fe (1 nmol L^{-1} ^{55}Fe) bound to 10 μmol L^{-1} EDTA (high Fe treatment). Two bottles were prepared for size-fractionated Fe:C ratio measurements identically to the low Fe treatment, except that the bottles were also amended with $NaH^{14}CO_3$ (NEN Life Sciences). The Fe-amended bottles were incubated in on-deck incubators at in situ light levels (corresponding to 10 m depth) and temperature (~13.5°C) that were controlled using neutral density screening and continuously flowing surface seawater, respectively. After a 24-hour incubation, 3 L of seawater were filtered through a stack of Poretics® polycarbonate filters of 0.2, 0.8 and 8 μm porosity, separated with Millipore® drain disk filters. These filter porosities were chosen to exclude grazers such as ciliates by retaining them on the 8.0-μm filter, and to separate phytoplankton (including *Synechococcus*) (0.8–8.0 μm) from heterotrophic bacteria (0.2–0.8 μm). Before running dry, the filters were rinsed with 0.2-μm filtered Ti(III) citrate EDTA solution [*Hudson and Morel*, 1989] to dissolve any extracellular Fe, followed by a rinsed with 0.2-μm filtered seawater. The biomass on the 0.8-μm and 0.2-μm filters was then resuspended in 10 mL of 0.2-μm filtered seawater to prepare radiolabeled cell concentrates (picophytoplankton and bacteria, respectively).

2.9.2. Grazing Experiments

[21] The radiolabeled cell concentrates were diluted in 500 mL of 200-μm-filtered seawater and incubated in the dark for 24 hours. In each experiment, treatments were performed in duplicate. Control treatments consisted of resuspended ^{55}Fe-labeled cells in 0.2-μm-filtered seawater and were used to correct Fe regeneration data for factors other than grazing (e.g., cell lysis). At T_{24}, ~500 mL of sample was collected on 0.2-, 0.8- and 2.0-μm porosity polycarbonate filters rinsed with Ti(III) citrate EDTA solution. One-milliliter samples of unfiltered and <0.2-μm-filtered seawater were collected for the determination of total and dissolved Fe, respectively. Each bottle was sampled at T_0 and T_{24} for enumeration of heterotrophic bacteria, *Synechococcus* and eukaryotic phytoplankton using flow cytometry. Samples were also taken at T_0 for the enumeration of heterotrophic flagellates and ciliates. Cell "concentrates" were added to incubation bottles at abundances approximating those in situ; in the herbivory experiments, abundances were virtually identical to in situ conditions (*Synechococcus* = $1.7 \times 10^5 - 2.5 \times 10^5$ cells mL^{-1}; eukaryotes = 16,800–19,500 cells mL^{-1}). Initial and final concentrations of prey changed negligibly between T_0 and T_{24}, suggesting that grazing rates were closely coupled to algal and bacterial growth rates (data not shown), and that our manipulations did not result in appreciable cell lysis. In both bacterivory experiments, the abundance of radiolabeled bacteria was around 46% of that in situ (1.0×10^6

Table 2. A Steady State Microbial Fe Budget for FeCycle[a]

Plankton	Abundance, cells mL^{-1}	Biomass,[b] $\mu mol\ C\ L^{-1}$	Fe:C,[c] $\mu mol\ mol^{-1}$	Biogenic Fe, $pmol\ L^{-1}$	Turnover Rate,[d] d^{-1}	Steady State Fe Uptake Rate, $pmol\ L^{-1}\ d^{-1}$	Regeneration Rate of Fe,[e] $pmol\ L^{-1}\ d^{-1}$	Total Biogenic Fe Demand, $pmol\ L^{-1}\ d^{-1}$	Total Biogenic Fe Supply,[f] $pmol\ L^{-1}\ d^{-1}$
				Producers					
Eukaryotic phytoplankton (2.0–8.0 μm)	$1.7 \times 10^4 \pm 5.9 \pm 10^3$	1.2 ± 0.2	2	2.4	0.34–1.07	0.81–2.54		26.2–101	31.5–43.9
Autotrophic flagellates (0.8–2.0 μm)	$1.1 \times 10^3 \pm 4.6 \times 10^2$	1.0 ± 0.4	8	7.8	0.23–1.27	1.8–9.9			
Synechococcus (0.8–2.0 μm)	$1.7 \times 10^5 \pm 3.1 \times 10^4$	3.5 ± 0.6	19	67.1	0.33–1.26	22.2–84.6			
Heterotrophic bacteria (0.2–0.8 μm)	$2.3 \times 10^6 \pm 3.3 \times 10^5$	3.8 ± 0.6	7.5	28.4	0.05–0.15	1.4–4.3			
				Microzooplankton					
Ciliates	4.6 ± 1.1	0.53 ± 0.12	11.6	6.2					
Heterotrophic flagellates	$3.7 \times 10^2 \pm 1.6 \times 10^2$	0.24 ± 0.11	11.6	2.8					
Total microzooplankton		0.78 ± 0.13		8.9			15.0–25.5 from bacteria, 16.5–18.4 from phytoplankton		
Total		10.2		114.5					
Virus	$4–84 \times 10^7$	0.7–14[g]	nd	nd		nd	0.4–28	nd	nd

[a]The budget format is based on work by *Bowie et al.* [2001], with the inclusion of additional microbial components such as virus-like particles. Here nd denotes no data.

[b]Biomass was calculated using mixed layer average cell abundance and published conversion factors (see text). Units for viral biomass are nmol C L^{-1}.

[c]In all cases, Fe:C ratios are taken either from steady state Fe-limited laboratory cultures, or direct measures of Fe-limited cells using nonradiotracer techniques. The Fe:C ratios were taken from the following sources: 1, Eukaryotic phytoplankton: four species of Southern Ocean phytoplankton (R. Strzepek, unpublished data, 2004); 2, autotrophic flagellates [*Twining et al.*, 2004; *Maranger et al.*, 1998]; 3, *Synechococcus* [*Brand*, 1991], assuming a Fe:P ratio of $10^{-2.7}$ and a C:P ratio of 106; 4, heterotrophic bacteria [*Tortell et al.*, 1996]; 5, heterotrophic flagellates [*Chase and Price*, 1997; *Twining et al.*, 2004]; and 6, ciliates: no literature values were found. We therefore used the values for heterotrophic flagellates.

[d]Turnover rates for eukaryotic phytoplankton and heterotrophic bacteria range from those estimated by *Bowie et al.* [2001] for Southern Ocean populations to those calculated from average mixed layer production (eukaryotic algae: 2.0–5.0 μm fraction) and abundance measurements. The lower limit for *Synechococcus* was determined from dilution experiments; the upper limit was calculated from mixed layer production (0.2–2.0 μm fraction) and abundance measurements. The lower limit for autotrophic flagellates is from *Bowie et al.* [2001]; the upper limit is from dilution experiments.

[e]Lower limit of Fe regeneration rates is that directly measured in grazing experiments. The upper limit was calculated by multiplying the calculated in situ biogenic Fe pool by the proportion of Fe regenerated into the dissolved phase (<0.2 μm) during grazing experiments (see Figure 3 and Table 1).

[f]Viral data were not included in our estimate of total biogenic Fe supply.

[g]Denotes nmol C L^{-1} to the DOC pool.

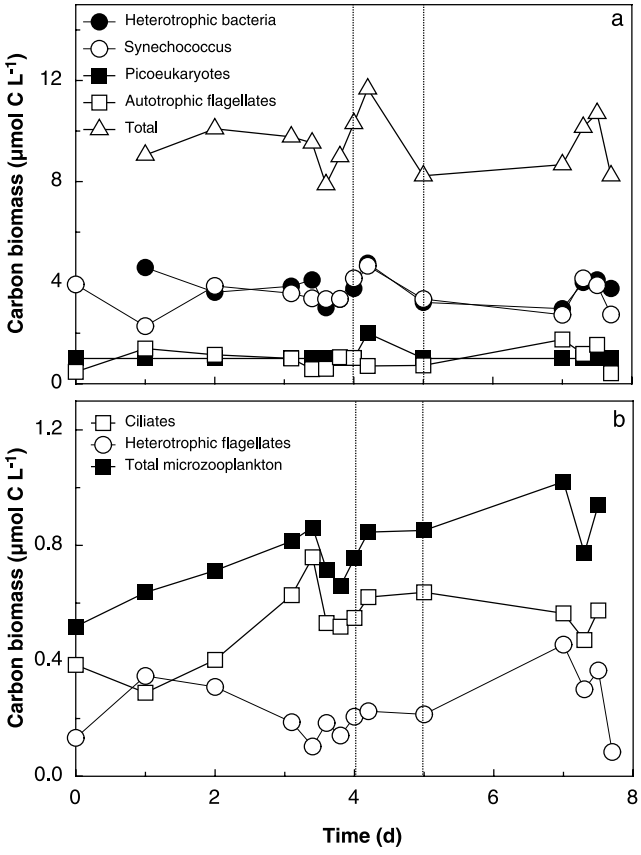

Figure 1. Carbon biomass estimates during FeCycle. All samples were collected from 10–20 m depth at the center of the SF_6 labeled patch. (a) Heterotrophic bacteria, autotrophic bacteria (*Synechoccocus*), autotrophic flagellates, and picoeukaryotes. (b) Microzooplankton. Carbon biomass was calculated from cell abundances and published conversion factors (see section 2). Dotted lines indicate the days during FeCycle when samples were collected for Fe regeneration experiments.

versus 2.3×10^6 cells mL^{-1}). To correct for this, we have multiplied the results (i.e., Fe content, biogenic Fe pool, and flux from Fe pool, Table 1) from these experiments by two (see section 2.10).

2.10. Caveats and Scaling Issues

[22] 1. The removal of extracellularly bound Fe [*Hudson and Morel*, 1989] in our prey-labeling experiments probably impacted on aspects of our microbial Fe budget. It is now acknowledged that both intracellularly and extracellularly bound Fe must be considered in developing Fe budgets [*Twining et al.*, 2004]. During FeCycle we may have underestimated the mobilization of Fe due to grazing by as much as 90% [*Tovar-Sanchez et al.*, 2003].

[23] 2. In the prey-labeling experiment we assumed that heterotrophic bacteria dominated the 0.2–0.8 μm size fraction, whereas the 0.8–8 μm fraction was dominated by phytoplankton. During FeCycle, flow cytometry revealed that both picophytoplankton (only *Synechococcus* were observed) and eukaryotic phytoplankton were always >1 μm, and heterotrophic bacteria were always submicron in size (J. Hall, unpublished data, 2004). This size threshold was used to separate cyanobacteria and bacteria, although some cells <1 μm may have been retained on filters of >1-μm porosity. Our grazer-mediated Fe recycling rates do not include the influence of herbivory on cells >8 μm.

[24] 3. In both bacterivory experiments, we scaled our results by a factor of 2 to take into account differences between the bacterial biomass in vitro and in situ. This scaling probably oversimplifies the predator-prey relationship with respect to grazing efficiency and prey concentration [*Strom et al.*, 2000].

[25] 4. During FeCycle we concurrently measured Fe uptake and C fixation, and estimated Fe:C ratios during radiotracer experiments in which we perturbed the Fe concentrations of the sampled HNLC waters. In the construction of our microbial Fe budget we opted to scale the budget (Table 2) for the steady state (unperturbed) conditions present during FeCycle. Difficulties in estimating the Fe:C ratios of members of the in situ community meant that, like previous studies, we relied on measures obtained from steady state Fe-limited laboratory cultures. For example, for eukaryotic algae we used data on diatom cultures isolated from HNLC waters (R. Strzepek, unpublished data, 2004) and in situ measurements of unperturbed cells from other HNLC systems. The implications of using "unperturbed" Fe:C ratios, rather than Fe:C ratios derived from our "perturbed" radiotracer experiments, in the budget are explored, as is the issue of scaling the results from such perturbations to obtain estimates of rates in HNLC waters (see section 4).

[26] 5. In the Fe budget we employed mean values for both biomass and rates for the microbial components, as there was little change in the magnitude of these terms during FeCycle (Figures 1 and 2). We have used published abundance to biomass algorithms in this budget (see section 2.2). The turnover rates of the various microbial pools are expressed as a range representing the upper and lower bounds, since these rates could be obtained using different approaches and Fe:C ratios.

3. Results

3.1. Microbial Biomass, Production, and Growth

[27] During FeCycle, the total plankton C in the mixed layer was nearly constant over our 10-day occupation of the SF_6-labeled patch (Figure 1). Typical of HNLC regions [*Boyd et al.*, 1995], C biomass was dominated by small cells, mainly prokaryotes (~90% of phytoplankton) (Figure 1a). In general, the total prokaryotic C biomass was partitioned equally between heterotrophic and autotrophic (*Synechococcus*) bacteria (~5 μmol C L^{-1} each). In contrast, eukaryote biomass was approximately fivefold lower (~1 μmol C L^{-1} for picoeukaryotes, autotrophic flagellates, $\ll$1 μmol C L^{-1} for diatoms and dinoflagellates [*McKay et al.*, 2005]) than for each of the prokaryote groups. Microzooplankton biomass was 0.5–1.0 μmol C L^{-1} and dominated by ciliates and, to a lesser extent, flagellates (Figure 1b). Total carbon biomass (~12 μmol C L^{-1}) was nearly identical to particulate organic carbon (POC) measured by *Frew et al.* [2005], supporting previous reports that detritus contributes little to the POC pool in

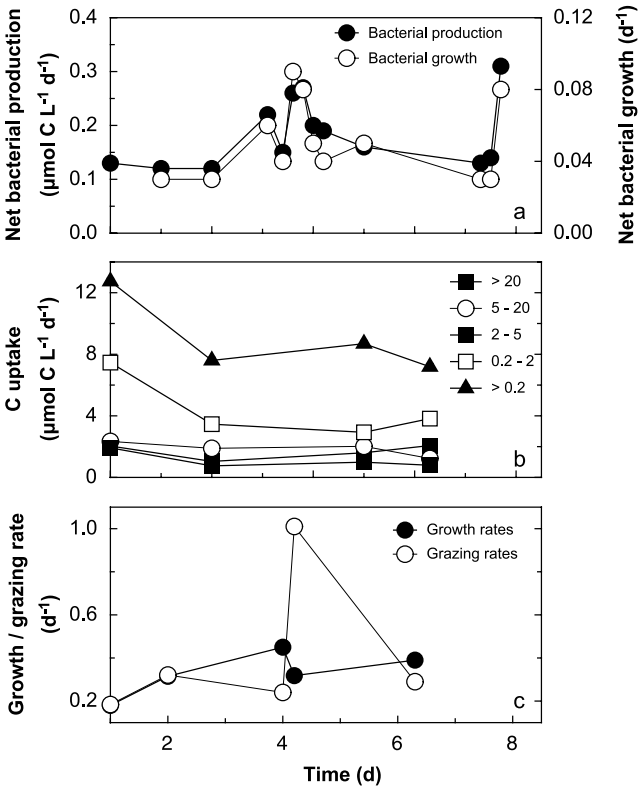

Figure 2. Rate estimates during FeCycle. (a) Net bacterial production and derived growth rates. (b) Size-fractionated C fixation obtained from 24-hour in situ incubations [see *McKay et al.*, 2005]. Unit for size fractions is μm. (c) Community (>0.2 μm) growth and grazing rates from dilution grazing experiments (see section 2).

HNLC regions [*Boyd et al.*, 1995; *Wheeler*, 1993]. Virus abundance was variable, ranging 20-fold from 4.1×10^7 (day 1 and 4) to 8.4×10^8 particles mL^{-1} (days 7 and 9), despite relatively constant bacterial abundance. On the basis of a published carbon conversion factor [*Wilhelm and Suttle*, 1999], viruses contributed between 0.68 and 14.0 nmol C L^{-1} to the dissolved organic carbon pool.

[28] Bacterial and phytoplankton production were relatively uniform during FeCycle (Figure 2). Despite the high bacterial biomass, net bacterial production was remarkably low, ranging from 0.1 to 0.3 μmol C L^{-1} d^{-1} (Figure 2a). Consequently net bacterial growth rates (d^{-1}), estimated from bacterial biomass and net production, were slow (0.02 to 0.08 d^{-1}). The 0.2–2.0 μm size fraction accounted for 34–59% of primary production, while the remainder was partitioned equally amongst the larger size fractions (Figure 2b). Thus, while *Synechococcus* and heterotrophic bacteria were of comparable biomass, *Synechococcus* had considerably higher production rates (with the caveat that some indirect uptake of DIC (i.e., via algal exudation of $DO^{14}C$ over the 24-hour incubation) in this fraction was by heterotrophic bacteria). However, vertical profiles showed that both C fixation and Fe uptake rates by the 0.2–2.0 μm size fraction decreased substantially with depth [*McKay et al.*, 2005], consistent with the majority of C fixation being due to *Synechococcus*. Growth rates of *Synechococcus* ranged from 0.3 to 1.3 d^{-1}, as estimated independently from grazing experiments, and C fixation rates and biomass, respectively. The results of grazing experiments generally suggested that algal growth was closely coupled to grazing rates (Figure 2c), as is characteristic of HNLC regions [*Landry et al.*, 1993].

[29] Estimates of virus production rates were highly variable during FeCycle. Virus-like particle production rates ranged 50-fold from 0.18 to 9.8×10^4 particles mL^{-1} h^{-1}. Burst size also varied (29.8 ± 10.9, n = 14), but to a lesser extent than virus-like particle production rates. Consequently, the calculated Fe remobilization rates due to viral lysis ranged from 0.4–1.2 pM Fe d^{-1} (day 1 and 4) to 16–28 pM d^{-1} (day 7 and 9).

3.2. Grazer Regeneration Experiments: Partitioning of Iron Between Size Fractions

[30] We observed a striking difference in the partitioning of Fe depending on whether microzooplankton were fed labeled bacteria or phytoplankton (Figure 3). When bacteria were the prey, over 90% of the Fe was regenerated to the dissolved (<0.2 μm) fraction and only 10% remained in the bacterial fraction (Figure 3a). In contrast, in herbivory experiments, only 25% of the Fe was regenerated into the dissolved phase while the remainder was retained in the phytoplankton fraction (Figure 3b). This difference in Fe partitioning between bacteria- and phytoplankton-fed grazers was observed in two independent experiments, and under both low (1 nM Fe: 10 μM EDTA) and high (20 nM Fe: 10 μM EDTA) Fe conditions. Furthermore, ~100% of the added tracer was recovered, as indicated by the close agreement between measures of total Fe in unfractionated seawater sample and the sum of filtered fractions (Figure 3). Duplicate samples for each treatment were in close agreement (range ±12.1% of the average). Between 1.4 ± 0.4% (herbivory) and 3.6 ± 0.3% (bacterivory) of total Fe was observed in the dissolved (<2.0 μm) fraction in control treatments (i.e., in the absence of grazers), confirming there was no significant Fe release from prey via other processes (e.g., cell lysis).

3.3. Iron Regeneration Experiments: Pools and Fluxes

[31] In each experiment, the absolute sizes of the Fe pools differed between heterotrophic bacteria and phytoplankton (Table 1). The phytoplankton Fe pool, which was comprised of the 2.0–8.0 μm (eukaryotic autotrophs) and 0.8–2.0 μm (mainly *Synechococcus* and some picoeukaryotes) fractions, was threefold larger than the heterotrophic bacterial Fe pool (60–66 pmol L^{-1} versus 18–19 pmol L^{-1}). As the C biomass of the heterotrophic bacteria and *Synechococcus* were comparable, this result was due solely to the greater cellular Fe requirement of *Synechococcus* compared to heterotrophic bacteria. Consequently, despite the greater proportion of Fe (<0.2 μm) regenerated from bacterivory compared to herbivory, the absolute fluxes of Fe from these sources to the dissolved phase was nearly identical (Table 1).

3.4. Microbial Fe Budget for FeCycle

[32] A steady state microbial Fe budget (Table 2) was constructed using data obtained during FeCycle (e.g., cell abundance, biomass, turnover rates and regeneration rates),

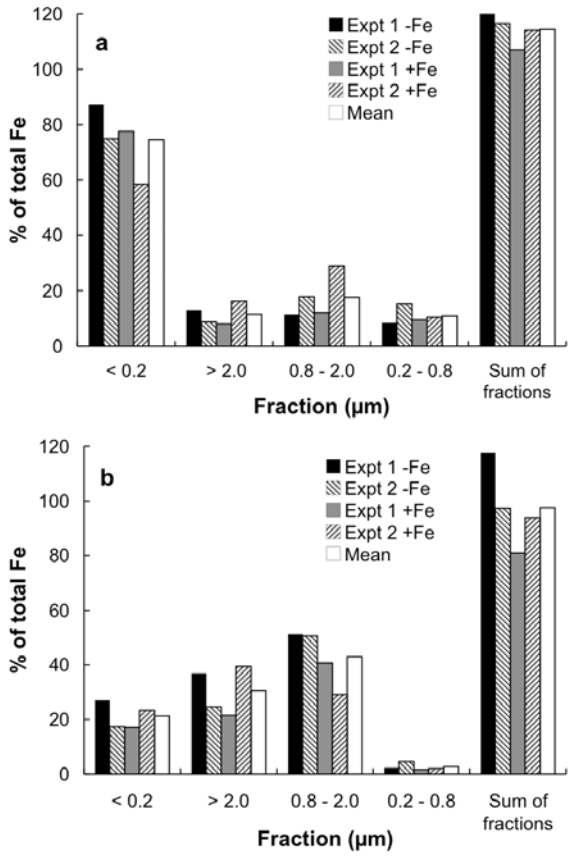

Figure 3. The size partitioning of ^{55}Fe label (initially within labeled prey) after ~24 hours in the presence of micro-grazers. (a) Bacterivory experiments: heterotrophic bacteria (0.2 to 0.8 μm) were labeled with ^{55}Fe for 24 hours and added to seawater containing resident microzooplankton. (b) Herbivory experiments: phytoplankton (0.8 to 8.0 μm) were labeled with ^{55}Fe for 24 hours and added to seawater containing resident microzooplankton. +Fe treatment denotes prey that were labeled in a medium containing 20 nM Fe bound to 10 μM EDTA. −Fe treatment denotes prey that were labeled in a medium containing 1 nM Fe bound to 10 μM EDTA. The dissolved fraction is denoted by <0.2 μm, bacterial fraction by 0.2–0.8 μm, picophytoplankton by 0.8–2 μm, and eukaryotic phytoplankton by >2μm size classes.

and Fe:C ratios reported for lab cultures grown under steady state Fe limitation [e.g., *Brand*, 1991] or for cells in HNLC regions using non-tracer techniques [*Twining et al.*, 2004]. As in the prey-labeling experiments, the budget results suggest that while heterotrophic bacteria and *Synechococcus* are the dominant C pools, *Synechococcus* is the largest biogenic Fe pool owing to its significantly higher cellular Fe requirement. Turnover rates of *Synechococcus* were also approximately tenfold higher than heterotrophic bacteria (0.33–1.26 versus 0.05–0.15 d^{-1}, respectively). Consequently, we calculate that the steady state Fe uptake rates (i.e., Fe-demand) of *Synechococcus* (22.2–84.6 pmol L^{-1} d^{-1}) are 20-fold greater than those of heterotrophic bacteria and eukaryotic phytoplankton (1.8–9.9 and 1.4–4.3 pmol L^{-1} d^{-1}, respectively). Our budget calculations also suggest that Fe regenerated via grazing alone is sufficient to supply between 30% (based on the upper bound of Fe demand, lower bound of Fe supply) and >100% (lower bound of Fe demand) of the biogenic Fe demand of algal and bacterial communities.

[33] In this budget, the role of viruses is less clear, as Fe regeneration rates due to bacteria cell lysis ranged from 0.4 pM d^{-1} to 28 pM d^{-1} (i.e., 1 to 64% of grazer-mediated regeneration rates). The transition observed between days 1 to 4 and days 7 to 9 in virus activity during FeCycle makes it difficult to incorporate viruses into a "steady state" model. As such the results may illustrate that steady state within a system may not apply to all of the biologically components equally [*Hutchinson*, 1961]. It is also not possible to define the relative contributions of Fe regeneration due to virus and grazer activity.

4. Discussion

[34] Our main findings on the composition and the fluxes within the microbial foodweb, such as carbon fixation and the dominance of picoplankton, are similar to those reported in spring and summer for a locale 30 nautical miles south of the FeCycle site [*Bradford-Grieve et al.*, 1999]. Thus our results are broadly representative of these subantarctic HNLC waters in summer. FeCycle provides the first estimates of virus-like particle abundance and production rates in surface HNLC waters south of New Zealand. Estimates of virus abundance ranged from 0.23 to 8.2 × 10^8 mL^{-1} in the center of the FeCycle patch over 10 days, with the majority of the estimates being between 1 and 3 × 10^8 mL^{-1}. These lower estimates from FeCycle are toward the upper bound in abundances reported for other waters [*Wilhelm et al.*, 2003; *Weinbauer*, 2004], but are comparable with those measured from HNLC waters, off the coast of Peru, by *Poorvin et al.* [2004].

4.1. Partitioning of Biogenic Iron During FeCycle

[35] The pools of biogenic Fe for each component of the microbial foodweb are presented in Figure 4. In subantarctic waters, prokaryotes dominated C biomass (Table 2) and constituted the largest biogenic Fe pool (83%, Figure 4). These results are qualitatively similar to the pelagic budget calculations of *Tortell et al.* [1999] for NE subarctic Pacific HNLC waters and the northern Sargasso Sea. However, our results differ in several key aspects. The total biogenic Fe pool for HNLC waters at the FeCycle site (115 pmol L^{-1}) is 3.5 to 6.8 larger than for the NE Pacific (16.9 pmol L^{-1} [*Tortell et al.*, 1999]; 33 pmol L^{-1} [*Price and Morel*, 1998]), and approximately double that reported for the oligotrophic Sargasso Sea (41–48 pmol L^{-1}, heterotrophic grazers excluded) by *Tortell et al.* [1999]. Our biogenic Fe pool estimates are also around fourfold larger than that measured, a few days after the onset of the SOIREE mesoscale Fe enrichment, in polar HNLC waters (27.09 pmol L^{-1}, mesozooplankton excluded [*Bowie et al.*, 2001]). The major reason for this difference between our budget and previous calculations from other HNLC systems is the high *Synechococcus* biomass observed during FeCycle, which was approximately tenfold greater than that for the NE Pacific and Sargasso Sea [*Tortell et al.*, 1999]. *Synechoco-*

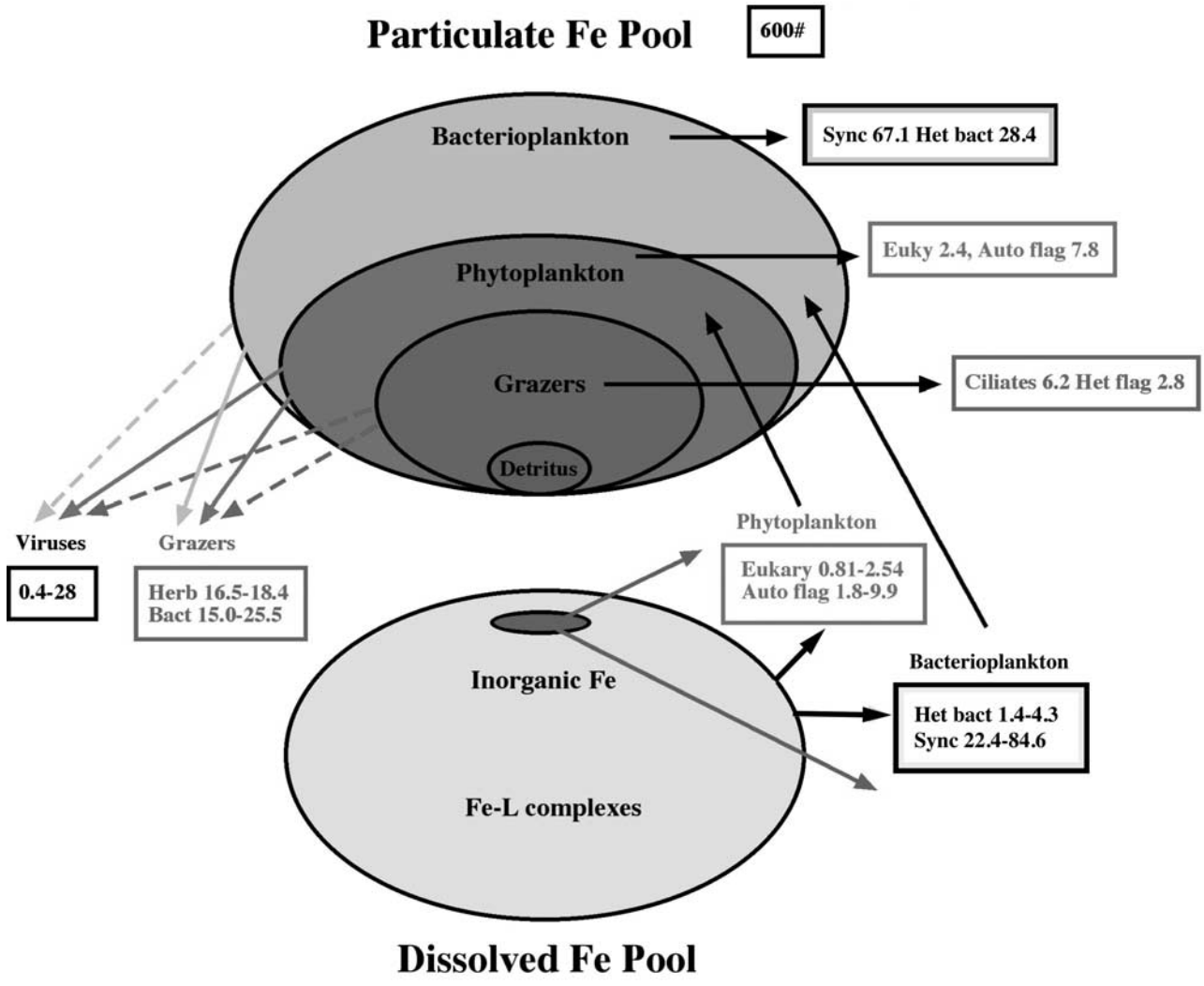

Figure 4. A schematic of the subantarctic HNLC microbial Fe budget for the surface mixed layer, based on the Fe budget presented in Table 2. Pools (denoted by horizontal arrows and adjacent boxes) are in pmol Fe L^{-1}, and rates (denoted by downward arrows (regeneration) or upward (demand) arrows, are in pmol Fe L^{-1} d^{-1}. Dashed arrows denote pathways that were not examined during FeCycle, such as viral lysis of phytoplankton. The $600^{\#}$ denotes PFe; 80% of PFe was lithogenic [*Frew et al.*, 2005]. Total biogenic Fe was 115 pmol Fe L^{-1}. See color version of this figure at back of this issue.

ccus are not present in the polar Southern Ocean, presumably due to low temperature [*Boyd*, 2002].

[36] The total biogenic Fe that we calculated (115 pmol L^{-1}) is around 15% of the 600 pmol L^{-1} total particulate Fe (PFe) for the mixed layer measured by *Frew et al.* [2005]. Frew et al. indicate that the lithogenic Fe pool (based on an Fe:Al crustal abundance molar ratio for Australian dust of 0.18) made up ~80% of the total PFe pool (i.e., biogenic Fe is around 0.12 nmol L^{-1}). *Price and Morel* [1998] also report a PFe of 560 pmol L^{-1} for the HNLC NE subarctic Pacific, but they estimated that the lithogenic pool was 30% (using an 0.33 Fe:Al molar ratio) with the detrital Fe pool being >50% (calculated by difference). In contrast, during FeCycle there is a strong suggestion that the detrital pool is small relative to the biogenic and lithogenic Fe pools, as discussed by *Frew et al.* [2005]. The microbial regeneration of Fe appears to be an extremely important Fe source compared to inputs of "new" Fe, with a calculated "*f*e" ratio (uptake of new iron/uptake of new + regenerated iron) of 0.09 [*Boyd et al.*, 2005]).

4.2. Microbial Iron Demand

[37] In addition to contributing substantially to total biogenic Fe, prokaryotes, particularly *Synechococcus*, appear to assimilate a large fraction of the dissolved Fe during FeCycle. Steady state Fe uptake rates calculated from the total Fe in each biological pool and calculated turnover rates from FeCycle suggest that cyanobacteria alone account for 83% of total community uptake. In contrast, despite the high C biomass of heterotrophic bacteria, they have a very slow turnover rate (estimated from biomass and production rates) and a correspondingly low Fe demand (1–5% of total). These calculations are supported by direct measurements of

size-fractionated ^{55}Fe uptake rates that show that ~57% of the total volumetric uptake rates is due to prokaryotic algae (0.2–2.0 μm) [*Maldonado et al.*, 2005]. When normalized to C biomass, Fe uptake rates for prokaryotes are significantly faster, by 3- to 60-fold, depending on the experimental treatment, than those of eukaryotic algae [*Maldonado et al.*, 2005]. The total Fe demand (26–101 pmol L^{-1} d^{-1}; Table 2) during FeCycle is considerably higher than the 3 pmol L^{-1} d^{-1} estimated (using the product of the average rate of turnover and the Fe content of plankton from lab cultures) for the NE subarctic Pacific [*Price and Morel*, 1998], or the Fe demand of 11.9 pmol L^{-1} d^{-1} (using ^{55}Fe) for polar waters during SOIREE [*Bowie et al.*, 2001].

4.3. Microbial Fe Supply During FeCycle

[38] The ability of microzooplankton to regenerate Fe from prey is well documented, both in the laboratory [*Barbeau and Moffett*, 2000; *Barbeau et al.*, 2001] and in the field [*Hutchins et al.*, 1993; *Bowie et al.*, 2001]. Our experiments showed a fundamental difference in how Fe was regenerated, depending on whether the prey were heterotrophic bacteria or phytoplankton (Table 1, Figure 3). Our results suggest that although *Synechococcus* constitutes a much larger Fe pool than heterotrophic bacteria, the proportion of this pool that is regenerated by microzooplankton is substantially lower (25% versus 90%). Consequentially, the supply of Fe from bacterivory and herbivory (including *Synechococcus*) were virtually identical (Table 2). This grazer-mediated recycled supply of Fe of 31.5 to 43.9 pmol L^{-1} d^{-1} compares to estimates of 5.0 pmol L^{-1} d^{-1} for the NE subarctic Pacific [*Price and Morel*, 1998], and 9.8 pmol L^{-1} d^{-1} for Fe regeneration by both micro- and meso-zooplankton in HNLC Southern Ocean waters at the onset of SOIREE [*Bowie et al.*, 2001].

[39] Taking Fe demand and supply (from grazers) together, the FeCycle budget calculations suggest that Fe regenerated via grazing could supply between 30 and >100% of the biogenic Fe demand in subantarctic waters. This Fe supply term will be conservative as it does not include Fe recycling from extracellularly bound Fe (see section 2.10), supply due to herbivory on cells >8 μm, or virus activity. However, the herbivory (on cells >8 μm) term is likely to be small as these cells comprised <20% of the algal biomass [*McKay et al.*, 2005]. The elevated Fe supply and demand terms reported for FeCycle, compared with other HNLC regions, may be due in part to the higher chlorophyll concentrations we encountered (0.6 μg chl L^{-1} compared to ~0.3 μg chl L^{-1} for the NE subarctic Pacific [*Price and Morel*, 1998; *Tortell et al.*, 1999] or polar Southern Ocean [*Bowie et al.*, 2001]. Despite marked differences between the magnitude of Fe supply and demand between the published budgets for the NE subarctic Pacific [*Price and Morel*, 1998] and the polar Southern Ocean [*Bowie et al.*, 2001], in each case there is good agreement between the magnitude of biological Fe demand and supply.

4.4. Grazer Versus Virus-Mediated Fe Supply

[40] One of the aims of FeCycle was to quantify the relative roles of grazer and virus-mediated Fe regeneration, as the latter also play a potentially important role in Fe supply in HNLC waters [*Poorvin et al.*, 2004]. Our Fe supply results in Table 2 indicate that virus-mediated Fe supply ranged by several orders of magnitude during FeCycle, with the lower and upper bounds of virus-mediated Fe supply being significantly less and greater than that supplied by grazers, respectively. The role of viruses in Fe regeneration has only be studied in the field by *Poorvin et al.* [2004], who reported regeneration rates of 19–75 pmol Fe L^{-1} d^{-1} in HNLC waters off Peru, i.e., more consistent with the upper bound observed in FeCycle.

[41] Owing to the wide range of rates of virus-mediated Fe regeneration, we have not included them in our microbial Fe budget (Table 2). The reasons for the observed hundredfold range in rates of Fe regeneration by viruses may include sample handling and processing, which may have influenced the accuracy of some estimates [*Wen et al.*, 2004], and rapid fluctuations in the abundance of virus-like particles. Although we sampled seawater for virus studies around the same time (0600 to 0700 hours) each day, populations of virus-like particles in surface waters are reported to be dynamic and have been shown to vary by twofold to fourfold within periods of only 10–20 min [*Bratbak et al.*, 1996]. Such variability is thought to be due to the sensitivity of viruses to both the chemistry of the water column and to ambient irradiances, the major factor destroying viruses in surface waters [*Wilhelm et al.*, 1998].

[42] The rates of virally mediated Fe regeneration increased dramatically between day 4 and day 7 of FeCycle. During this period there was an increase in chlorophyll concentrations in the patch [*McKay et al.*, 2005] that was probably due to the lateral entrainment of higher chlorophyll waters into the patch [*Boyd et al.*, 2005]. As obligate pathogens, viruses function through what is referred to as the "kill the winner" hypothesis [*Thingstad and Lignell*, 1997]: as infection of hosts is strictly controlled by virus-host contacts, and the frequency of these contacts is proportional to the abundance of both the virus and host cells [*Murray and Jackson*, 1992]. Thus the entrainment of additional chlorophyll (i.e., more host cells) and/or viruses into the patch may have resulted in increased virus infection (and subsequent lysis) within this community. As illustrated here and in other studies of viruses and trophic structure [*Dean et al.*, 2005] these shifts occur rapidly.

[43] The upper bound of virus-mediated Fe regeneration rates (90 pmol Fe L^{-1} d^{-1}) would account for the majority of the algal and bacterial Fe demand during FeCycle (Table 2). However, due to the wide variability in regeneration rates it remains unclear as to how important this pathway is in resupplying Fe. Future studies need to conduct high-resolution sampling (minutes) to better define the diel cycle of virus-mediated Fe regeneration rates. Moreover, they should investigate the forms of the Fe being regenerated, relative to grazers, as it has been proposed that virus-mediated regeneration of Fe results in the release of organically complexed Fe whereas grazing releases "both organic and (primarily) inorganic Fe" [*Poorvin et al.*, 2004].

4.5. Fate of Labeled Fe During Grazer Experiments

[44] The ^{55}Fe radiotracer budget for both the bacterivory and herbivory experiments in FeCycle displayed different

trends with respect to the partitioning of the label. In the former the majority of the label was in the dissolved phase (<0.2 μm) after T_{24} with a small proportion in each of the three particulate fractions. In the latter 20% or less was in the dissolved phase, with around 50% being in the >0.8-μm fraction (i.e., the fraction containing the originally labeled phytoplankton). These experiments were conducted in the presence of resident (i.e., nonradiolabeled) bacteria and phytoplankton that could potentially take up this regenerated Fe in the dissolved pool. This likely occurred in the herbivory experiments, as the rates of Fe acquired from in situ ligands by the resident population were comparable to rates of Fe regenerated via herbivory (24.2–50.6 versus 16.5–18.4 pmol L^{-1} d^{-1}, respectively [*Maldonado et al.*, 2005]). That appreciable uptake of regenerated Fe from the dissolved pool did not occur in the bacterivory experiment suggests that the regenerated Fe may not have been bioavailable since microbes have developed several acquisition mechanisms to obtain Fe in HNLC waters [*Morel and Price*, 2003]. In the herbivory experiment, there was threefold smaller proportion of Fe in the dissolved pool after 24 hours, compared to the bacterivory experiment. This may indicate that the Fe released was more bioavailable and/or that bacterivory releases a higher proportion of Fe than herbivory.

[45] Previous studies of grazer-mediated trace metal cycling using lab cultures have reported that the regenerated metals (Gd, Cs, Cd and Zn) were less available for resorption by phytoplankton (cyanobacteria) than were these metals in the initial inorganic growth medium (where the metals were in equilibrium with inorganic ligands) [*Twiss and Campbell*, 1995]. Twiss and Campbell reported that this enigma might be due to the release of organic ligands (dissolved or colloidal) associated with microzooplankton digestion. *Barbeau et al.* [2001] examined the recycling of Fe by heterotrophic flagellates grazing on heterotrophic bacteria in a lab culture. They also reported that a substantial proportion of the Fe mobilized by grazing was found in the dissolved phase and that bacterivory resulted in the formation of ''relatively stable dissolved and colloidal metal organic species.''

[46] Although the experiments in FeCycle were conducted using HNLC water with the resident plankton present, an approach advocated by *Barbeau et al.* [2001], as opposed to a laboratory monoculture of either heterotrophic bacteria or picophytoplankton [*Twiss and Campbell*, 1995; *Barbeau et al.*, 2001], the trends were similar in both experimental approaches. During FeCycle, there was little change in dissolved Fe or Fe-binding ligand concentrations (Croot et al., submitted manuscript, 2005), high rates of both bacterivory and herbivory were observed (Figure 2) and the resident phytoplankton were able to obtain Fe bound to a wide range of Fe-binding ligands [*Maldonado et al.*, 2005]. Thus it is unclear why no increase in dissolved Fe concentrations, associated with the reduced availability of Fe following grazer-mediated regeneration, was observed in FeCycle. It is possible that we encountered an experimental artifact due to timescales of the tracer kinetics [see *Geider*, 1988] in relation to the duration of our experiment, such that we observed a pulse of regenerated Fe (this will be dependent on gut residence times) before it was taken up. Future experiments should address this by running time-course experiments that track the pools and fluxes of Fe with greater resolution. Such studies should also measure the speciation of Fe in the dissolved phase, which could resolve the nature of the Fe released to the dissolved phase, and provide insights into whether the regenerated Fe is bound to different types of natural ligands, depending on the prey [*Hutchins et al.*, 1999; *Barbeau et al.*, 2001]. These measurements may also provide insights into the nature and degree of complexation of different cellular pools (i.e., metabolically functioning Fe versus Fe stored in a non-metabolic pool).

[47] It is also not possible to comment on the different trends in Fe partitioning into size classes in our prey-labeling experiments, as we have no information on predator-prey interactions within each size class. For example, the >2-μm fraction will contain plankton with a wide range of trophic modes, from autotrophy to omnivory. We can say, however, that either the rate of Fe regeneration from bacteria is substantially faster compared to picophytoplankton, or that the Fe regenerated from bacteria is substantially less bioavailable than Fe regenerated from picophytoplankton.

4.6. Scaling Issues: Perturbation or Amplification?

[48] In order to measure the pathways of Fe via regeneration, we had to perturb the system by adding Fe, in excess of ambient, in labeling and other experiments to study specific processes within the Fe biogeochemical cycle, such as Fe uptake and or grazer-mediated regeneration. Such short-term Fe additions have been acknowledged to result in the luxury uptake of Fe, i.e., higher than ambient uptake rates [e.g., *Schmidt and Hutchins*, 1999]. Do such additions result in perturbation or in amplification effects in the exploration of these specific biogeochemical pathways?

[49] Several lines of evidence suggest that during our experiments such Fe additions amplified rather than perturbed these pathways. First, the rates of Fe regeneration estimated for steady state conditions (by multiplying the total biogenic Fe pool by the proportion liberated via grazing) and the direct measures from grazing experiments agree remarkably well (Table 2). Second, the proportion of Fe liberated via grazing was identical in low and high Fe grazing experiment treatments, despite a 20-fold difference in Fe'. However, some aspects of Fe biogeochemistry appear to be particularly sensitive to Fe additions. This is best illustrated by comparing the Fe:C ratios obtained during a range of treatments (a 20-fold range in Fe concentrations) during FeCycle with ratios measured during steady state Fe limited growth (Table 3). The 20-fold range of Fe added (expressed as Fe′) reveals a greater than tenfold increase in Fe:C ratios with increasing Fe enrichment. This trend was observed for all size fractions during such shipboard Fe enrichments on FeCycle. (For heterotrophic bacteria, these high Fe:C ratios may also be due, in part, to limited labeling of cells with ^{14}C, as $H^{14}CO3$- must first cycle through the autotrophic component prior to being assimilated as $DO^{14}C$). A similar trend has been reported by *Twining et al.* [2004], who compared planktonic Fe:C ratios prior to and during the mesoscale SOFEX polar Fe enrichment. Although such short-term Fe additions appear to

Table 3. Summary of Molar Fe:C Ratios From Studies Using Steady State Fe-Limited Laboratory Cultures, Compared With Fe:C Ratios Obtained by a Variety of Approaches on FeCycle and Prey-Labeling Micrograzer Experiments[a]

Experiment	Iron addition	Labeling Period	Group/Fraction	Fe:C, μmol mol^{-1}
Steady state laboratory cultures	rate limiting	generations	eukaryotic phytoplankton	2
			autotrophic flagellates	9
			Synechococcus	19
			heterotrophic bacteria	7.5
PFe: POC	none (DFe ~ 50 pmol L^{-1}) Fe′ = 0.2–1.0 pmol L^{-1}	n/a	total	41.7
In situ incubations (n = 8)	2 nM Fe: 20 μM EDTA Fe′ = 5.0 pmol L^{-1}	24 hours	>20 μm	3.1 ± 1.1
			5.0–20	4.8 ± 1.6
			2.0–5.0	8.8 ± 2.6
			0.2–2.0	18.3 ± 6.4
			>0.2 (total)	12.1 ± 3.2
Micrograzer (−Fe) (n = 8)	1 nM Fe: 10 μM EDTA Fe′ = 5.0 pmol L^{-1}	24 hours	<0.2 (dissolved)	5.0–8.2
			>2.0 (nanophytoplankton)	22–31
			0.8–2.0 (*Synechococcus*)	59–188
			0.2–0.8 (heterotropic bacteria)	20–30
			total	7–21
Micrograzer (+Fe) (n = 8)	20 nM Fe: 10 μM EDTA Fe′ = 100 pmol L^{-1}	24 hours	<0.2 (dissolved)	36–50
			>2.0 (nanophytoplankton)	244–248
			0.8–2.0 (*Synechococcus*)	649–810
			0.2–0.8 (heterotropic bacteria)	90–227
			total	65–195

[a]FeCycle: suspended particulates and in situ incubations (^{55}Fe and ^{14}C, 7 depths [*McKay et al.*, 2005]). Laboratory data on eukaryotic phytoplankton, autotrophic flagellates, *Synechococcus*, and heterotrophic bacteria were derived from R. Strzepek (unpublished data on HNLC diatom cultures, 2004), *Maranger et al.* [1998], *Brand* [1991], and *Tortell et al.* [1996], respectively.

represent amplification (defined here as altered physiological rates, no floristic shift) rather than perturbation (floristic shifts, altered physiological rates such as Si:NO_3 uptake stoichiometry [*Takeda*, 1998]), these results illustrate the difficulty in applying or scaling such rates to ambient HNLC conditions.

[50] In the absence of sufficient data on the pools and fluxes in the biogeochemical cycle of Fe, Fe:C ratios have been used extensively by biogeochemical modelers [*Moore et al.*, 2002], geo-engineers (assessing the efficacy of ocean Fe fertilization as an atmospheric CO_2 mitigation strategy [*Buesseler and Boyd*, 2003]), and to construct regional Fe budgets [*Landry et al.*, 1996]. For example, the Fe budget presented in Table 2 attempts to represent ambient HNLC conditions by using published Fe:C ratios from unperturbed conditions (either steady state lab cultures under limiting Fe conditions, or from SXRF (synchrotron-based X-ray fluorescence) analysis in field studies). Clearly, care in the use of such ratios by modelers is required, given that ratios will vary with the degree Fe enrichment (Table 3, this study, and *Twining et al.* [2004]), steady state versus nonsteady state, whether intracellular and/or externally bound Fe is considered [*Tovar-Sanchez et al.*, 2003], and the manner in which other particulate Fe pools (such as lithogenic or detrital) are calculated [see *Frew et al.*, 2005]. The use of Fe:C ratios from a range of approaches would result in some dramatic alterations in the estimates for biogenic Fe and subsequent calculations of Fe turnover rate and steady state uptake rate. This would result in a severalfold elevation of algal and bacterial Fe demand, which are key terms in the microbial Fe budget.

5. Summary

[51] 1. The microbial foodweb is responsible for rapid Fe regeneration (hours to days) in the upper ocean. Between 30 and >100% of biological Fe demand is met by grazer-mediated Fe regeneration. Both herbivory and bacterivory regenerate similar amounts of Fe. However, we could not establish the relative contribution of grazer and virus activity to Fe regeneration in steady state HNLC waters as viral Fe regeneration rates varied 100-fold. Such fluctuations are thought to be due in part to rapid changes (on timescales of minutes) in virus-like particle abundance. Nevertheless, the microbial foodweb plays a key role in rapidly recycling much of the Fe required by plankton in the upper ocean.

[52] 2. Tracer-labeling experiments suggest that the fate of the Fe released from labeled prey differs for herbivory compared to bacterivory. There is some suggestion that the released Fe that enters the dissolved Fe pool is less bioavailable than dissolved Fe complexed to strong binding ligands in the HNLC ocean; however, this may be due to experimental artifacts such as tracer kinetics.

[53] 3. A wide range of Fe:C ratios were obtained during FeCycle, with the magnitude of the ratios being determined by the degree of Fe enrichment, radioisotope studies versus particle analysis, and whether the particulate Fe was corrected for both the lithogenic pool and/or extracellularly bound Fe. As current biological Fe budgets rely heavily on Fe:C ratios, care is needed in selecting appropriate ratios for such budget.

[54] **Acknowledgments.** We thank the officers and crew on the NIWA research vessel RV *Tangaroa*, and the personnel at NIWA vessel services. This research was funded in part by the New Zealand PGSF Ocean Ecosystems project.

References

Azam, F., T. Fenchel, J. G. Field, J. S. Gray, L. A. Meyer-Reil, and F. Thingstad (1983), The ecological role of water-column microbes in the sea, *Mar. Ecol. Prog. Ser.*, *10*, 257–263.

Barbeau, K., and J. W. Moffett (2000), Laboratory and field studies of colloidal iron oxide dissolution as mediated by phagotrophy and photolysis, *Limnol. Oceanogr.*, *45*, 827–835.

Barbeau, K., J. W. Moffett, D. A. Caron, P. L. Croot, and D. L. Erdner (1996), Role of protozoan grazing in relieving iron limitation of phytoplankton, *Nature*, *380*, 61–64.

Barbeau, K., E. B. Kujawinski, and J. W. Moffett (2001), Remineralization and recycling of iron, thorium and organic carbon by heterotrophic marine protists in culture, *Aquat. Microb. Ecol.*, *24*, 69–81.

Berges, J. A., D. J. Franklin, and P. J. Harrison (2001), Evolution of an artificial seawater medium: Improvement in enriched seawater, artificial water over the last two decades, *J. Phycol.*, *37*, 1138–1145.

Bidle, K. D., M. Manganelli, and F. Azam (2002), Regulation of oceanic silicon and carbon preservation by temperature control on bacteria, *Science*, *298*, 1980–1984.

Bloem, J., M. B. Bar-Gilissen, and T. E. Cappenberg (1986), Fixation counting and manipulation of heterotrophic nano-flagellates, *Appl. Environ. Microbiol.*, *52*, 1266–1272.

Booth, B. C. (1988), Size classes and major taxonomic groups of phytoplankton at two locations in the subarctic ocean in May and August, 1984, *Mar. Biol.*, *97*, 275–286.

Bowie, A. R., M. T. Maldonado, R. D. Frew, P. L. Croot, E. P. Achterberg, R. F. C. Mantoura, P. J. Worsfold, C. S. Law, and P. W. Boyd (2001), The fate of added iron during a mesoscale fertilisation in the Southern Ocean, *Deep Sea Res., Part II*, *48*, 2703–2744.

Boyd, P. W. (2002), Environmental factors controlling phytoplankton processes in the Southern Ocean, *J. Phycol.*, *38*, 844–861.

Boyd, P. (2004), Ironing out algal issues in the Southern Ocean, *Science*, *304*, 396–397.

Boyd, P. W., S. Strom, F. A. Whitney, S. Doherty, M. E. Wen, P. J. Harrison, C. S. Wong, and D. E. Varela (1995), The NE subarctic Pacific in winter: Biological standing stocks, *Mar. Ecol. Prog. Ser.*, *128*, 11–24.

Boyd, P. W., et al. (2005), FeCycle: Attempting an iron biogeochemical budget from a mesoscale SF6 tracer experiment in unperturbed low iron waters, *Global Biogeochem. Cycles*, doi:10.1029/2005GB002494, in press.

Bradford-Grieve, J. M., P. W. Boyd, F. H. Chang, S. Chiswell, M. Hadfield, J. A. Hall, M. R. James, S. D. Nodder, and E. A. Shuskina (1999), Pelagic ecosystem structure and functioning in the Subtropical Front region east of New Zealand in austral winter and spring 1993, *J. Plankton Res.*, *21*, 405–428.

Brand, L. (1991), Minimum iron requirements of marine-phytoplankton and the implications for the biogeochemical control of new production, *Limnol. Oceanogr.*, *36*, 1756–1771.

Bratbak, G., M. Heldal, T. Thingstad, and P. Tuomi (1996), Dynamics of virus abundance in coastal seawater, *FEMS Microbiol. Ecol.*, *19*, 263–269.

Buesseler, K. O., and P. W. Boyd (2003), Will ocean fertilization work?, *Science*, *300*, 67–68.

Chang, F. H. (1988), Distribution, abundance and size composition of phytoplankton off Westland, New Zealand; February 1982, *N. Z. J. Mar. Freshwater Res.*, *22*, 345–367.

Chase, Z., and N. M. Price (1997), Metabolic consequences of iron deficiency in heterotrophic marine protozoa, *Limnol. Oceanogr.*, *42*, 1673–1684.

Coroz, A., F. Jimenez-Gomez, F. J. L. Gordillo, R. Garcia-Ruiz, and F. X. Niell (1999), *Synechnococcus* and *Prochlorococcus*-like populations detected by flow cytometry in a eutrophic reservoir in summer, *J. Plankton Res.*, *21*, 1575–1581.

Dean, A. L., J. L. Higgins, J. M. DeBruyn, J. M. Rinta-Kanto, R. A. Bourbonniere, and S. W. Wilhelm (2005), Viral populations in Lake Erie: Abundance, production and predicted impacts, *Aquat. Ecosyst. Health Manage.*, in press.

de Baar, H. J. W., and P. W. Boyd (1999), The role of iron in plankton ecology and carbon dioxide transfer of the global oceans, in *The Dynamic Ocean Carbon Cycle: A Midterm Synthesis of the Joint Global Ocean Flux Study*, *Int. Geosphere Biosphere Programme Book Ser.*, edited by R. B. Hanson et al., chap. 4, pp. 61–140, Cambridge Univ. Press, New York.

Ducklow, H. W., and C. A. Carlson (1992), Oceanic bacterial production, *Adv. Microb. Ecol.*, *12*, 113–181.

Frew, R. D., D. A. Hutchins, S. Nodder, S. Sanudo-Wilhelmy, A. Tovar-Sanchez, and P. W. Boyd (2005), Particulate iron dynamics during FeCycle in subantarctic waters southeast of New Zealand, *Global Biogeochem. Cycles*, doi:10.1029/2005GB002558, in press.

Fuhrman, J. A., and F. Azam (1982), Thymidine incorporation as a measure of heterotrophic bacterial production in marine surface waters: Evaluation and field results, *Mar. Biol.*, *66*, 109–120.

Fukuda, R., H. Ogawa, T. Nagata, and I. Koike (1998), Direct determination of carbon and nitrogen contents of natural bacterial assemblages in marine environments, *Appl. Environ. Microbiol.*, *64*, 3352–3358.

Fung, I. Y., S. K. Meyn, I. Tegen, S. C. Doney, J. G. John, and J. K. B. Bishop (2000), Iron supply and demand in the upper ocean, *Global Biogeochem. Cycles*, *14*, 281–296.

Gallegos, C. L., W. N. Vant, and K. A. Safi (1996), Microzooplankton grazing of phytoplankton in Manukau Harbour, New Zealand, *N. Z. J. Mar. Freshwater Res.*, *30*, 423–434.

Geider, R. J. (1988), Estimating the growth and loss rates of phytoplankton from time-series observations of ^{14}C-bicarbonate uptake, *Mar. Ecol. Prog. Ser.*, *30*, 85–92.

Hall, J. A., K. Safi, and A. Cumming (2004), Role of microzooplankton grazers in the subtropical and subantarctic waters east of New Zealand, *N. Z. J. Mar. Freshwater Res.*, *38*, 91–101.

Hobbie, J. E., R. J. Daley, and S. Jasper (1977), Use of nuclepore filters for counting bacteria by fluorescence microscopy, *Appl. Environ. Microbiol.*, *33*, 1225–1228.

Hudson, R. J. M., and F. M. M. Morel (1989), Distinguishing between extra- and intracellular iron in marine phytoplankton, *Limnol. Oceanogr.*, *34*, 1113–1120.

Hutchins, D. A., and K. W. Bruland (1994), Grazer-mediated regeneration and assimilation of Fe, Zn and Mn from planktonic prey, *Mar. Ecol. Prog. Ser.*, *110*, 259–269.

Hutchins, D. A., G. R. DiTullio, and K. W. Bruland (1993), Iron and regenerated production: Evidence for biological iron recycling in two marine environments, *Limnol. Oceanogr.*, *38*, 1242–1255.

Hutchins, D. A., A. E. Witter, A. Butler, and G. W. Luther (1999), Competition among marine phytoplankton for different chelated iron species, *Nature*, *400*, 858–861.

Hutchinson, G. E. (1961), The paradox of the plankton, *Am. Nat.*, *95*, 137–145.

James, M. R., and J. A. Hall (1995), Planktonic ciliated protozoa: Their distribution and relationship to environmental variables in a marine coastal ecosystem, *J. Plankton Res.*, *17*, 659–683.

Kirchman, D. L. (1996), Microbial ferrous wheel, *Nature*, *383*, 303–304.

Landry, M. R., and R. P. Hasset (1982), Estimating the grazing impact of marine microzooplankton, *Mar. Biol.*, *67*, 283–288.

Landry, M. R., B. C. Monger, and K. E. Selph (1993), Time-dependency of microzooplankton grazing and phytoplankton growth in the subarctic Pacific, *Prog. Oceanogr.*, *32*, 205–222.

Landry, M. R., J. Kirshtein, and J. Constantinou (1996), Abundances and distributions of picoplankton populations in the central equatorial Pacific from 12°N to 12°S, 140°W, *Deep Sea Res., Part II*, *43*, 871–890.

Lebaron, P., N. Parthuisot, and P. Catala (1998), Comparison of blue nucleic acid dyes for flow cytometric enumeration of bacteria in aquatic systems, *Appl. Environ. Microbiol.*, *64*, 1725–1730.

Li, W. K., P. M. Dickie, B. D. Irwin, and A. M. Wood (1992), Biomass of bacteria, cyanobacteria, prochlorophytes and photosynthetic eukaryotes in the Sargasso Sea, *Deep Sea Res.*, *39*, 501–519.

Maldonado, M. T., R. F. Strzepek, S. Sander, and P. W. Boyd (2005), Acquisition of iron bound to strong organic complexes, with different Fe binding groups and photochemical reactivities, by plankton communities in Fe-limited subantarctic waters, *Global Biogeochem. Cycles*, *19*, GB4S23, doi:10.1029/2005GB002481.

Maranger, R., D. F. Bird, and N. M. Price (1998), Iron acquisition by photosynthetic marine phytoplankton from ingested bacteria, *Nature*, *396*, 248–251.

McKay, R. M. L., W. Wilhelm, J. Hall, D. A. Hutchins, M. M. D. Al-Rshaidat, C. E. Mioni, S. Pickmere, D. Porta, and P. W. Boyd (2005), Impact of phytoplankton on the biogeochemical cycling of iron in subantarctic waters southeast of New Zealand during FeCycle, *Global Biogeochem. Cycles*, doi:10.1029/2005GB002482, in press.

Moore, J. K., S. C. Doney, D. M. Glover, and I. Y. Fung (2002), Iron cycling and nutrient-limitation patterns in surface waters of the world ocean, *Deep Sea Res., Part II*, *49*, 463–507.

Morel, F. M. M., and N. M. Price (2003), The biogeochemical cycles of trace metals in the oceans, *Science*, *300*, 944–947.

Morel, F. M. M., J. G. Reuter, and N. M. Price (1991), Iron nutrition of phytoplankton and its possible importance in the ecology of ocean regions with high nutrient and low biomass, *Oceanography*, *4*, 56–61.

Murray, A. G., and G. A. Jackson (1992), Viral dynamics: A model of the effects of size, shape, motion and abundance of single-celled planktonic organisms and other particles, *Mar. Ecol. Prog. Ser.*, *89*, 103–116.

Noble, R. T., and J. A. Fuhrman (1998), Use of SYBR Green I for rapid epifluorescence counts of marine viruses and bacteria, *Aquat. Microb. Ecol.*, *14*, 113–118.

Pomeroy, L. R. (1974), The ocean's food web, a changing paradigm, *Bioscience*, *24*, 499–504.

Poorvin, L., J. M. Rinta-Kanto, D. A. Hutchins, and S. W. Wilhelm (2004), Viral release of Fe and its bioavailability to marine plankton, *Limnol. Oceanogr.*, *49*, 1734–1741.

Price, N. M., and F. M. M. Morel (1998), Biological cycling of iron in the ocean, in *Metal Ions in Biological Systems*, vol. 35, *Iron Transport and Storage in Micro-organisms, Plants and Animals*, pp. 1–36, CRC Press, Boca Raton, Fla.

Putt, M., and D. K. Stoecker (1989), An experimentally determined carbon—Volume ratio for marine oligotrichous ciliates from estuarine and coastal waters, *Limnol. Oceanogr.*, *34*, 1097–1103.

Sanders, R. W., K. G. Porter, S. J. Bennett, and A. E. De Biase (1989), Seasonal patterns of bacterivory by flagellates, ciliates, rotifers and cladocerans in a freshwater planktonic community, *Limnol. Oceanogr.*, *34*, 673–687.

Sandström, S., A. G. Ivanov, Y. I. Park, G. Öquist, and P. Gustafsson (2002), Iron stress responses in the cyanobacterium *Synechococcus* sp. pcc7942, *Physiol. Plant.*, *116*, 255–263.

Schmidt, M. A., and D. A. Hutchins (1999), Size-fractionated biological iron and carbon uptake along a coastal to offshore transect in the NE subarctic Pacific, *Deep Sea Res., Part II*, *46*, 2487–2504.

Schmidt, M. A., Y. Zhang, and D. A. Hutchins (1999), Assimilation of Fe and carbon by marine copepods from Fe-limited and Fe-replete diatom prey, *J. Plankton Res.*, *21*, 1753–1764.

Smith, D. C., and F. Azam (1992), Protein content and protein synthesis rates of planktonic marine bacteria, *Mar. Ecol. Prog. Ser.*, *51*, 201–213.

Strickland, J. D. H., and J. R. Parsons (1972), A practical handbook of seawater analysis, *Fish. Res. Board Can. Bull.*, *167*, 311 pp.

Strom, S. L., C. B. Miller, and B. W. Frost (2000), What sets lower limits to phytoplankton stocks in high nitrate, low chlorophyll regions of the open ocean?, *Mar. Ecol. Prog. Ser.*, *193*, 19–31.

Takeda, S. (1998), Influence of iron availability on nutrient consumption ratio of diatoms in oceanic waters, *Nature*, *393*, 774–777.

Thingstad, T. F., and R. Lignell (1997), Theoretical models for the control of bacterial growth rate, abundance, diversity and carbon demand, *Aquat. Microb. Ecol.*, *13*, 19–27.

Tortell, P. D., M. T. Maldonado, and N. M. Price (1996), The role of heterotrophic bacteria in iron-limited ocean ecosystems, *Nature*, *383*, 330–332.

Tortell, P. D., M. T. Maldonado, J. Granger, and N. M. Price (1999), Marine bacteria and biogeochemical cycling of iron in the oceans, *FEMS Microbiol. Ecol.*, *29*, 1–11.

Tovar-Sanchez, A., S. A. Sañudo-Wilhelmy, M. Garcia-Vargas, R. S. Weaver, L. C. Popels, and D. A. Hutchins (2003), A trace metal clean reagent to remove surface-bound iron from marine phytoplankton, *Mar. Chem.*, *82*, 91–99.

Twining, B. S., S. B. Baines, N. S. Fisher, and M. R. Landry (2004), Cellular iron contents of plankton during the Southern Ocean Iron Experiment (SOFeX), *Deep Sea Res., Part I*, *51*, 1827–1850.

Twiss, M. R., and P. G. C. Campbell (1995), Regeneration of trace metals from picoplankton by nanoflagellate grazing, *Limnol. Oceanogr.*, *40*, 1418–1429.

Verity, P. G., C. Y. Robertson, G. R. Tronzo, M. G. Andrews, J. R. Nelson, and M. E. Sieracki (1992), Relationships between cell volume and carbon and nitrogen content of marine photosynthetic nanoplankton, *Limnol. Oceanogr.*, *37*, 1434–1446.

Weinbauer, M. G. (2004), Ecology of prokaryotic viruses, *FEMS Microbiol. Rev.*, *28*, 127–181.

Weinbauer, M. G., and C. A. Suttle (1996), Potential significance of lysogeny to bacteriophage production and bacterial mortality in coastal waters of the Gulf of Mexico, *Appl. Environ. Microbiol.*, *62*, 4374–4380.

Welschmeyer, N. A. (1994), Fluorometric analysis of chlorophyll a in the presence of chlorophyll *b* and phaeopigments, *Limnol. Oceanogr.*, *39*, 1985–1992.

Wen, K., A. C. Ortmann, and C. A. Suttle (2004), Accurate estimation of viral abundance by epifluorescence microscopy, *Appl. Environ. Microbiol.*, *70*, 3862–3867.

Wheeler, P. A. (1993), New production in the subarctic Pacific Ocean: Net changes in nitrate concentrations, rates of nitrate assimilation and the accumulation of particulate nitrogen, *Prog. Oceanogr.*, *32*, 137–162.

Wilhelm, S. W., and C. A. Suttle (1999), Viruses and nutrient cycles in the sea, *BioScience*, *49*, 781–788.

Wilhelm, S. W., and C. G. Trick (1994), Iron-limited growth of cyanobacteria: Multiple siderophore production is a common response, *Limnol. Oceanogr.*, *39*, 1979–1984.

Wilhelm, S. W., M. G. Weinbauer, C. A. Suttle, and W. H. Jeffrey (1998), The role of sunlight in the removal and repair of viruses in the sea, *Limnol. Oceanogr.*, *43*, 586–592.

Wilhelm, S. W., S. M. Brigden, and C. A. Suttle (2002), A dilution technique for the direct measurement of viral production: A comparison in stratified and tidally mixed coastal waters, *Microb. Ecol.*, *43*, 168–173.

Wilhelm, S. W., W. H. Jeffrey, A. L. Dean, J. Meador, and D. L. Mitchell (2003), Ultraviolet radiation induced DNA damage in marine viruses along a latitudinal gradient, *Aquat. Microb. Ecol.*, *31*, 1–8.

P. W. Boyd and R. F. Strzepek, National Institute of Water and Atmosphere Centre for Chemical and Physical Oceanography, Department of Chemistry, University of Otago, 700 Cumberland Street N, P.O. Box 56, Dunedin, New Zealand. (pboyd@alkali.otago.ac.nz; roberts@alkali.otago.ac.nz)

J. Hall and K. Safi, National Institute of Water and Atmosphere, Hillcrest, Box 11-115, Hamilton, New Zealand. (j.hall@niwa.co.nz; k.safi@niwa.co.nz)

J. L. Higgins and S. W. Wilhelm, Department of Microbiology, University of Tennessee, Knoxville, TN 37996-0845, USA. (jhiggin1@utk.edu; wilhelm@utk.edu)

M. T. Maldonado, Department of Earth and Ocean Sciences, University of British Columbia, Vancouver BC, V6T 1Z4, Canada. (mmaldonado@eos.ubc.ca)

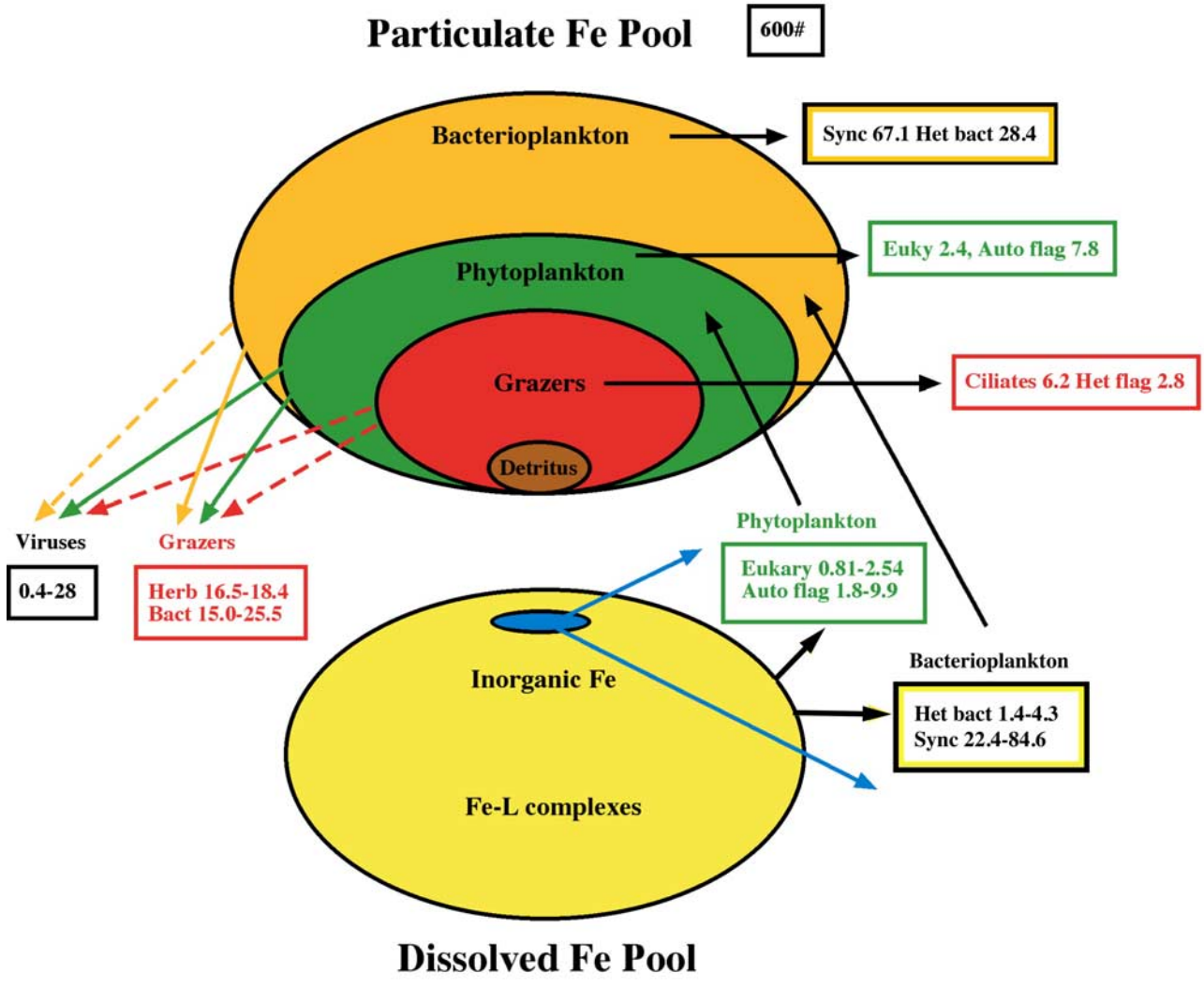

Figure 4. A schematic of the subantarctic HNLC microbial Fe budget for the surface mixed layer, based on the Fe budget presented in Table 2. Pools (denoted by horizontal arrows and adjacent boxes) are in pmol Fe L^{-1}, and rates (denoted by downward arrows (regeneration) or upward (demand) arrows, are in pmol Fe L^{-1} d^{-1}. Dashed arrows denote pathways that were not examined during FeCycle such as viral lysis of phytoplankton. The $600^{\#}$ denotes Pfe; 80% of PFe was lithogenic [*Frew et al.*, 2005]. Total biogenic Fe was 115 pmol Fe L^{-1}.